

Electronic structures and ferromagnetism of Cu- and Mn-doped ZnO

This article has been downloaded from IOPscience. Please scroll down to see the full text article.

2004 J. Phys.: Condens. Matter 16 4251

(<http://iopscience.iop.org/0953-8984/16/24/007>)

View [the table of contents for this issue](#), or go to the [journal homepage](#) for more

Download details:

IP Address: 129.252.86.83

The article was downloaded on 27/05/2010 at 15:34

Please note that [terms and conditions apply](#).

Electronic structures and ferromagnetism of Cu- and Mn-doped ZnO

Xiaobing Feng

Department of Physics, Dalian Railway Institute, Dalian 116028, People's Republic of China

Received 9 January 2004

Published 4 June 2004

Online at stacks.iop.org/JPhysCM/16/4251

doi:10.1088/0953-8984/16/24/007

Abstract

The electronic structures of magnetic orderings of $Zn_{1-x}TM_xO$ ($TM = Cu, Mn$) have been studied with the B3LYP hybrid density functional. The corrections for energy band dispersions with respect to the local density approximation (LDA) are similar to GW results, but lead to an improved energy gap. Cu and Mn are close to +2 valence in $Zn_{1-x}TM_xO$ ($TM = Cu, Mn$), but Cu^{1+} would be realized in n-type ZnO. Cu- and Mn-doped ZnO have ferromagnetic and antiferromagnetic ground states, respectively. Magnetic couplings between transition metal ions depend sensitively on the interatomic distance.

1. Introduction

The discovery of ferromagnetic ordering at temperature as high as 110 K in the diluted magnetic semiconductor (DMS) (Ga, Mn)As [1] has inspired intensive research on the room temperature ferromagnetic DMSs [2], which are expected to play an important role in spintronics [3]. In addition to the III–V based DMSs, oxide semiconductors, such as ZnO [4] and TiO_2 [5], have also been intensively studied due to their unique properties. Because of their wide band gaps these materials have important application in optoelectronic devices using short wavelength light. Transparent magnets may also be obtained by doping these wide-gap oxide semiconductors.

It is theoretically predicted that semiconducting materials with wide gaps, such as ZnO and GaN, could have high Curie temperatures when doped with transition metal (TM) elements [6]. The experimental results on the ferromagnetism in ZnO doped with TM elements have diverged. Ferromagnetic ordering with a Curie temperature ranging from 30 to 550 K has been reported in $Zn_{1-x}Co_xO$ ($T_c > 350$ K) [7], $(Zn, Sn)_{1-x}Mn_xO$ ($T_c \sim 250$ K) [8], $Zn_{0.7}Mn_{0.3}O$ ($T_c = 45$ K) [9], $Zn_{0.94}Fe_{0.05}Cu_{0.01}O$ ($T_c \sim 550$ K) [10], $Zn_{0.85}(Co_{0.5}Fe_{0.5})_{0.15}O$ ($T_c > 300$ K) [11] and $Zn_{0.85}Co_{0.15}O$ ($T_c \sim 300$ K) [12]. However, no ferromagnetism has been detected in $Zn_{0.75}Co_{0.25}O$ [13], $(Zn, Al)_{1-x}TM_xO$ ($TM = Cr, Mn, Fe, Co, Ni, Cu$) [14], $Zn_{0.64}Mn_{0.36}O$ [15] and $Zn_{1-x}TM_xO$ ($TM = Cr, Mn, Ni$) [12]. Spin-glass behaviour and

antiferromagnetic coupling between TM ions have been reported in [13, 15]. The quality of the samples depends sensitively on the preparation methods and the growth conditions. The diversity in the experimental results may be caused by impurity phases and ferromagnetic precipitates. Therefore, it is helpful to conduct a theoretical study with first-principle methods. Theoretically, changes of the electronic structure, spin density distribution, magnetic ordering and clustering effects can be conveniently studied without the complexity encountered in experimentally determining the origin of ferromagnetism. The first theoretical simulation with the local density approximation (LDA) has shown that ferromagnetism could be obtained in V-, Cr-, Fe-, Co- and Ni-doped ZnO [16]. In (Zn, Mn)O the antiferromagnetic state has a lower energy than the ferromagnetic one, but it may become a ferromagnetic semiconductor when holes are introduced. For Ti- and Cu-doped ZnO the ferromagnetic and antiferromagnetic states have nearly the same total energies [16]. A ferromagnetic and nearly half-metallic ground state is predicted with LDA for Fe and Co codoped ZnO [17]. The LDA calculations by Spaldin [18] show that no robust ferromagnetism could be obtained by doping Co or Mn, but additional holes can stabilize ferromagnetic states. There is no consensus on the ferromagnetism in ZnO doped with TM elements. More experimental and theoretical work is needed to clarify the situation. Mizokawa *et al* [19] have conducted photoemission spectroscopy measurements on $Zn_{1-x}Mn_xO$ and configuration-interaction calculations on a MnO_4 cluster model. The 3d on-site Coulomb interaction U is estimated to be 5.2 eV, which is comparable to the 6.0 eV in MnO. That means the correlation effects would play an important role in the electronic and magnetic properties of Mn-doped ZnO. For most semiconductors the energy gaps are underestimated by over 30% by LDA, and for some strongly correlated electronic systems the ground states are not correctly predicted by LDA. A theoretical scheme, which better takes the correlation effects into account, should be employed.

In this paper we study the electronic structures and possible ferromagnetic orderings in Mn- and Cu-doped ZnO with the B3LYP hybrid density functional method [20]. Mn has been one of the most often used dopants. Enhanced ferromagnetism could be found in some DMSs by codoping Cu [10]. The B3LYP method has been successfully applied to semiconductors of different bonding types and some strongly correlated electronic systems [21–27], such as Si, GaAs, diamond, MgO, Al_2O_3 , MnO, NiO, TiO_2 , ZnS, $CaCuO_2$, La_2CuO_4 and $LaMnO_3$. For these semiconducting or insulating antiferromagnetic materials, energy gaps and magnetic moments are in good agreement with experiments. B3LYP can predict the correct ground states of strongly correlated electronic systems [22, 23, 25–27], in which the 3d electrons play an important role in the electronic structure near the Fermi energy. B3LYP presents a significant improvement over LDA, which usually underestimates the energy gaps of semiconductors by over 30% and fails to predict the correct ground states of some correlated electronic systems, such as FeO, CoO and parent compounds of high temperature superconductors. For silicon the dispersion of the energy bands from the B3LYP scheme is in good agreement with experiment and is comparable to the quantum Monte Carlo and the GW approaches [21].

The calculation by Muscat *et al* [21] has shown that the energy gap of ZnO, among other semiconductors, is in excellent agreement with experiments. The result is much better than the other theoretical schemes, such as GW [28, 29], the local density approximation (LDA) [17, 28, 29] and LDA + U [17]. For DMSs the combination of the semiconducting hosts and the electron correlation on the transition metal ions renders the B3LYP method a promising theoretical scheme for the study of the electronic and magnetic properties of DMSs. To the best of our knowledge this is the first application of the B3LYP hybrid functional to a semiconductor doped with TM elements.

2. Calculation method

In the B3LYP hybrid density functional scheme the nonlocal Hartree–Fock (HF) is mixed into the total energy functional of the general gradient approximation (GGA) [20]. The argument for mixing the HF exchange into the exchange–correlation energy is based on the adiabatic connection formula [20]. The weights for the gradient-corrected correlation energy, local exchange energy and the nonlocal HF exchange were determined by a linear least-square fitting of the thermochemical properties of some atoms and molecules to experiments. 20% of the nonlocal HF exchange energy in the exchange–correlation energy gives theoretical results in good agreement with experiments. In the so-called B3LYP scheme the Perdew–Wang [30] gradient-corrected correlation energy, which was used in the original work of Becke, is replaced by the Lee–Yang–Parr correlation energy [31].

The admixture of HF exchange has important effects on the electronic and magnetic properties of materials, especially for correlated electronic systems. It has been realized that the success of the B3LYP functional in strongly correlated antiferromagnetic materials results from the reduction of the self-interaction due to the introduction of HF exchange. However, the removal of self-interaction alone is not enough to get good results for highly correlated systems, but the use of a better correlation energy is also essential to take the dynamical correlation effects into account. The successful application of the method to semiconductors, where self-interaction is not important, indicates that the B3LYP hybrid functional has a better description for the exchange and correlation energy than LDA and GGA.

The calculations are carried out with the CRYSTAL package [32]. The Kohn–Sham orbitals are expanded as linear combinations of atom-centred Gaussian basis sets [33]. All-electron basis sets for Zn, Cu and Mn ions are of the form of 86-411(41d)G. The basis set for the oxygen ion is of the form of 8-411G.

In the calculations for ZnO 65 points in the irreducible part of the first Brillouin zone were used. For calculations on periodic systems truncations have to be made in evaluating the bielectronic Coulomb and exchange integrals, which can be expressed as integrals involving Gaussian type functions on different atoms. The precision is controlled by five threshold parameters (ITOL1–ITOL5) in CRYSTAL [32]. The selection is performed according to overlap-like criteria: when the overlap between two atomic orbitals is smaller than $10^{-\text{ITOL}}$, the corresponding integral is disregarded or evaluated in a less precise way [32]. We adopt 7, 7, 7, 7 and 14 (default values are 6, 6, 6, 6 and 12) as the integral tolerances to obtain high precision in the bielectronic integrals. The convergence threshold exponent for the total energy is set to 7, which means that convergence is assumed when the total energy difference (in the atomic unit) for two consecutive iterations is less than 10^{-7} . A supercell of 32 atoms, which is obtained by doubling the three sides of the primitive cell, has been taken to study the doping effects in Cu- and Mn-doped ZnO. For comparisons, unrestricted HF (UHF) and LDA calculations for ZnO were also carried out with the same basis sets and precisions.

3. Results and discussion

3.1. Electronic structure of ZnO

In the first B3LYP calculation on ZnO only the energy gap was reported [21]. The energy bands from B3LYP and LDA along high symmetry lines in the first Brillouin zone of ZnO are shown in figure 1. The top of the valence bands is taken as reference energy. The conduction bands from the two schemes have nearly the same dispersions, but the conduction bands from B3LYP are shifted upwards by about 2 eV along all symmetry lines. This significantly improved the

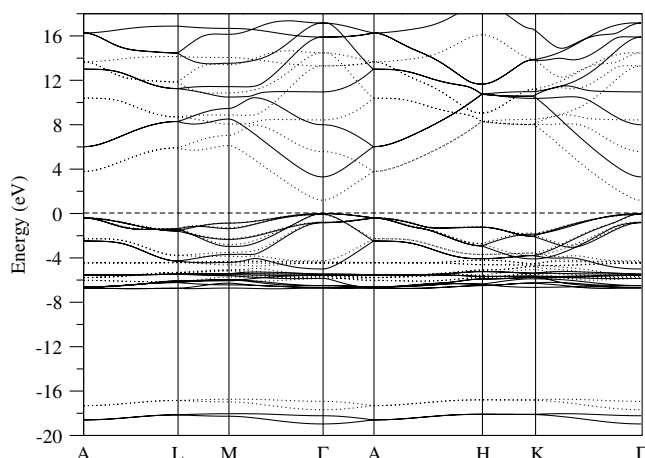


Figure 1. The B3LYP (solid curves) and LDA (dotted curves) energy bands along the high symmetry lines in the first Brillouin zone of ZnO.

Table 1. The energy gap (Δ , in eV) and core-level energies (E , in eV) of ZnO from various theoretical schemes are compared with experiments. For the core levels of Zn 3d and O 2s states the energy ranges are given for some theoretical approaches.

| | LDA | HF | LDA + U | GW | B3LYP | Expt |
|-------------|---|-----------------------------------|--------------------------------|-------------------------------------|------------------|----------------|
| Δ | 0.77 [28] 0.93 [29] 1.15 [34] 1.20 | 11.39 [28] 11.59 [29] 11.92 | 1.0 [17] | 2.44 [28] 4.23 [29] 4.28 [34] | 3.30 3.2 [21] | 3.3, 3.44 [34] |
| E (Zn 3d) | -3.0 to -5.0 [17] -5.4 [29] -4.4 | -11.4 [29] -9.2 to -10.4 | -6.0 to -7.0 [17] -6.4 [29] | -6.8 [28] | -5.2 to -6.8 | -8.8 [35] |
| E (O 2s) | -17.6 [29] -16.7 to -17.7 | -23.4 [29] -22.5 to -23.5 | | -18.6 [29] -18.7 [28] | -18.0 to -19.0 | -20.7 [35] |

agreement between the experimental energy gap and the theoretical one. One can see from table 1 that the theoretical energy gap from B3LYP is in good agreement with the experiments, and it is much better than the other theoretical approaches, such as GW [28, 29], LDA + U [17] and UHF. From the densities of states (DOSs) shown in figure 2 one can see that the gap is formed between O 2p and Zn 4s states. The Zn 3d states are well below the Fermi energy, so the Hubbard U , which is experienced by two 3d electrons on the same Zn ions, has little effect on the energy gap. That is why LDA + U shows hardly any improvement over the LDA energy gap. By taking into account part of the nonlocal and correlation effects, GW produced a much improved energy gap over both LDA and HF. However, the three reported GW gaps are all about 1 eV larger or smaller than the experiment. Usuda *et al* [28] pointed out that energy gaps are systematically underestimated by GW in semiconductors, with the errors increasing with ionicity. The B3LYP energy gap is closest to the experimental one.

From table 1 one can also see that B3LYP gives a significant improvement over the LDA results for the core-levels of Zn 3d and O 2s states. LDA underestimates the core-levels, while UHF overestimates them. The B3LYP results for the core-levels, which are close to the GW ones, are approximately the average values of the LDA and HF results. B3LYP produces similar

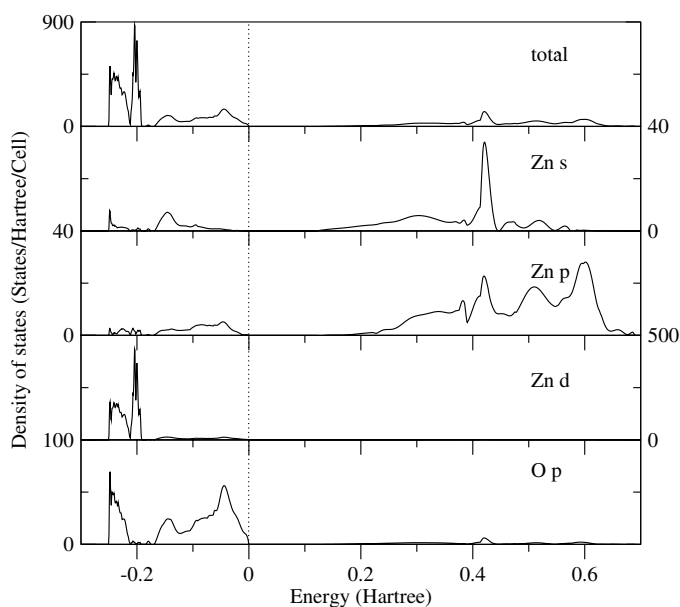


Figure 2. The densities of states (DOSs) for a ZnO supercell composed of eight primitive cells. The top of the valence bands is taken as reference energy.

corrections for the LDA quasiparticle energies as GW does, with the corrections being nearly independent of the wavevectors of quasiparticles. That means that the self-energy corrections by GW and B3LYP are mainly dependent on the energies. The dynamical mean-field theory could take the dynamical effects from the electronic correlations into account [36]. The self-energy correction depends only on the frequency. However, as pointed out before, in ZnO the Hubbard U has little effect on the electronic states near the Fermi energy. So, no significant improvement over the electronic structure of pure ZnO would be expected from this method.

3.2. Electronic structures of Cu- and Mn-doped ZnO

Some experimental [10] and theoretical [17] studies have shown that Cu could provide holes for ZnO doped with other transition metal elements, which helps increase the ferromagnetic transition temperature. Due to its high magnetic moment, Mn has been the most often used transition metal dopant for obtaining ferromagnetic semiconductors. The DOSs of Cu- and Mn-doped ZnO are shown in figures 3 and 4, respectively. From figures 3 and 4 one can see that Mn and Cu 3d orbitals have stronger hybridization with O 2p orbitals than Zn 3d. This is due to the fact that Mn and Cu 3d orbitals have higher energies than Zn 3d, i.e. the energy differences between Cu, Mn 3d orbitals and the O 2p states are smaller than the one between Zn 3d and O 2p. For Mn-doped ZnO the in-gap states, which are above the valence bands of ZnO, are formed from Mn 3d majority spin states. The energy gap is reduced to 2.05 eV for ferromagnetic $\text{Zn}_{0.875}\text{Mn}_{0.125}\text{O}$. B3LYP and LDA give crystal field splitting of nearly the same magnitude [18], but the exchange splitting from B3LYP (7.4 eV) is significantly larger than the one from LDA (about 4 eV) [18]. In LDA the strong Coulomb interaction between 3d electrons is not well taken into account due to the self-interaction inherent in LDA, which leads to incorrect metallic ground states for some antiferromagnetic insulating materials, such as FeO, CoO and parent high temperature superconductors. In B3LYP the self-interaction is

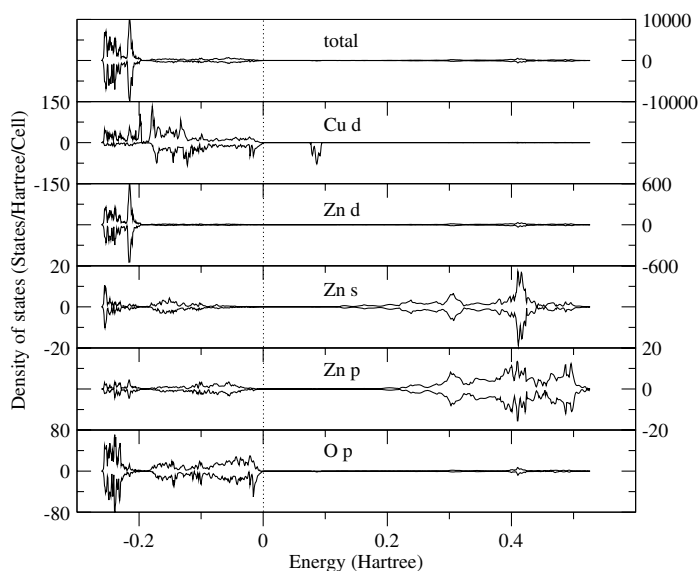


Figure 3. The B3LYP DOSs of Cu-doped ZnO. Positive and negative DOSs are for the spin-up and spin-down electrons, respectively. The supercell consists of eight primitive cells of ZnO, in which one Zn ion is substituted by Cu. Ferromagnetic ordering of Cu ions is assumed. The magnetic moment of Cu is $0.75 \mu_B$.

reduced by introducing HF exchange. This results in a larger exchange splitting than LDA. The total magnetic moment for a ferromagnetic supercell, which is doped with two Mn ions, is $10.00 \mu_B$, with most of the magnetic moment being located on Mn ions ($4.65 \mu_B$ for each Mn ion).

In Cu-doped ZnO the occupied Cu 3d states have strong hybridization with O p states. The unoccupied Cu 3d states are well separated from the occupied ones, with the energy gap being reduced to 2.03 eV for ferromagnetic $\text{Zn}_{0.9375}\text{Cu}_{0.0625}\text{O}$. In $\text{Zn}_{0.94}\text{Fe}_{0.05}\text{Cu}_{0.01}\text{O}$ the x-ray absorption spectroscopy measurement showed that the valence state of Cu is Cu^{1+} [10]. The Hall coefficient measurement has also shown that the number of carriers at room temperature had been reduced by doping with Cu [10]. However, in our B3LYP calculations the summed charge on Cu in $\text{Zn}_{0.9375}\text{Cu}_{0.0625}\text{O}$ is 27.35, which means that the valence of Cu in pure ZnO is close to +2 rather than +1. From figure 3 one can see that the unoccupied Cu 3d state is lower than the host conduction band states. So, for n-type ZnO the electrons would occupy the empty Cu 3d states leading to Cu^{1+} ions. This may be the mechanism for increased holes in ZnO codoped with Cu and other TM elements. Figure 4 shows that the unoccupied Mn 3d state is well above the lowest host conduction band states; therefore, the number of n-type carriers would not be reduced by doping with Mn. Actually, no hole-providing mechanism is found in Mn-doped ZnO.

3.3. Ferromagnetic ordering in Cu- and Mn-doped ZnO

Although Cu metal has no spontaneous magnetization, Cu ions can be spin polarized in some compounds, such as the CuO_2 planes in the high temperature superconductors. In search of a possible ferromagnetic ordering of Cu ions in ZnO we calculated the total energies for different magnetic configurations and different distances between the Cu ions, when two Zn ions are

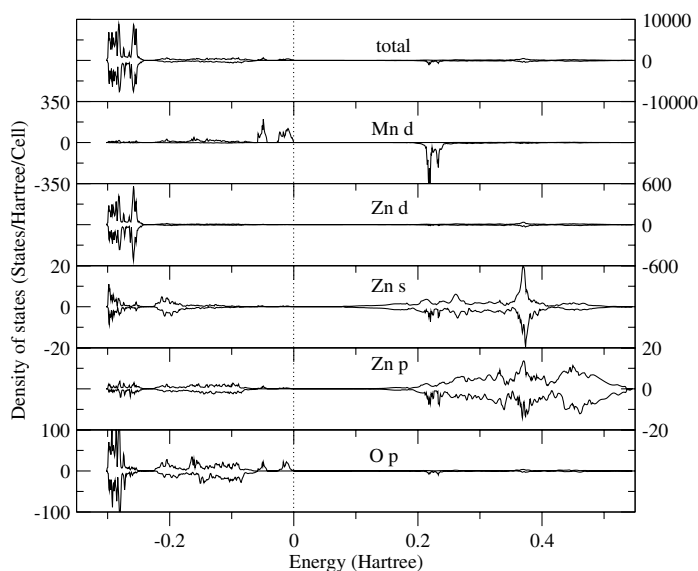


Figure 4. The B3LYP DOSs of Mn-doped ZnO. Positive and negative DOSs are for the spin-up and spin-down electrons, respectively. The supercell consists of eight primitive cells of ZnO, where two Mn ions are substituted for Zn ions along the *c*-axis. Ferromagnetic ordering of Mn ions is assumed. The Mn–Mn distance is 5.205 Å.

substituted with Cu ions. In one case ('far') the two Cu ions are well separated along the *c*-axis with a Cu–Cu distance of 5.205 Å; in the other case ('near') the two Cu ions are in the *ab* plane and have a distance of 3.249 Å, which is the shortest distance between two cations in the *ab* plane. The total energies of various configurations are given in table 2 from which the stable magnetic configuration can be acquired. From table 2 one can see that magnetic phases are more stable than the nonmagnetic ones. In the 'near' case the antiferromagnetic state is favoured over the ferromagnetic one, whereas in the 'far' case the ferromagnetic state has the lowest energy. Of all the magnetic configurations the ferromagnetic state with the largest distance between the two Cu ions has the lowest total energy, which means that ferromagnetic semiconductors can be obtained by doping Cu into ZnO. Our calculation also indicates that Cu-clustering is not stable in the ground state and it is detrimental to the ferromagnetism of Cu-doped ZnO. ZnO is an intrinsic n-type semiconductor: the electrons would occupy the Cu 3d states resulting in nonmagnetic Cu ions. So, ferromagnetism in Cu-doped ZnO would not be possible without additional hole doping.

For Mn-doped ZnO the energy differences between the magnetic phases and nonmagnetic states are much higher than the ones in Cu-doped ZnO. This is because a Mn^{2+} ion has five 3d electrons with parallel spins, so more energy is needed to flip half of the spins to make it a nonmagnetic ion. Our calculations show that $\text{Zn}_{0.875}\text{Mn}_{0.125}\text{O}$ has an antiferromagnetic ground state. This is in agreement with the experimental results that ferromagnetism is not obtained in several Mn-doped ZnO samples [14, 15, 12] and antiferromagnetic coupling between Mn ions was observed [15]. The $\text{Zn}_{0.875}\text{Mn}_{0.125}\text{O}$ with a shorter Mn–Mn distance has a lower total energy than the one with a larger Mn–Mn distance, supporting Mn clustering. However, some other experiments reported ferromagnetism in Mn-doped ZnO with low [8] and high [9] dopant concentrations. These experimental results are in disagreement with our B3LYP calculations and the LDA calculations by Sato *et al* [16]. The LDA results for $\text{Zn}_{0.75}\text{Mn}_{0.25}\text{O}$ showed that

Table 2. The energy (in eV) of various magnetic and nonmagnetic phases. The supercell is composed of eight ($2 \times 2 \times 2$) primitive cells; two TM (Cu, Mn) ions are substituted for two Zn ions. PM denotes a nonmagnetic state, or Pauli paramagnetic state, AFM an antiferromagnetic state, and FM a ferromagnetic state. In the ‘near’ case the TM–TM distance is 3.249 Å, which is the shortest distance between two cations in the *ab* plane of ZnO, while in the ‘far’ case the TM–TM distance is 5.205 Å and the two TM ions are aligned in the direction of the *c*-axis. The total energies of the PM state in the ‘far’ cases are taken as reference energies.

| | PM | AFM | FM |
|-----------|---------|--------|--------|
| Near (Cu) | −0.6398 | −2.032 | −1.363 |
| Far (Cu) | 0.0 | −2.042 | −2.055 |
| Near (Mn) | −1.097 | −8.535 | −8.367 |
| Far (Mn) | 0.0 | −8.396 | −8.407 |

the total energy of the antiferromagnetic state is about 0.2 eV lower than the ferromagnetic state. Our B3LYP calculations for the ‘near’ configuration gives a 0.17 eV energy difference between the ferromagnetic and the antiferromagnetic states. The difference between the LDA and B3LYP results may partly be caused from the different supercell sizes used in the LDA and B3LYP calculations.

Both in Cu- and Mn-doped ZnO the B3LYP calculations indicate that the magnetic couplings between TM ions sensitively depend on the TM–TM distances. Ferromagnetic coupling is found for the ‘far’ configuration, while an antiferromagnetic coupling is obtained for the ‘near’ configuration. This means that a homogeneous distribution of TM ions in ZnO would favour ferromagnetism. Cho *et al* [11] show that rapid thermal annealing leads to a remarkable increase in the spontaneous magnetization of the ZnO codoped with Co and Fe, and a significant increase in the Curie temperature. The thin films of diluted magnetic semiconductors are usually prepared using nonequilibrium methods, such as the low temperature molecular beam epitaxy method, which may produce inhomogeneous distributions of the magnetic ions. This may be one of the reasons why different experiments have reached quite different conclusions on the ferromagnetism in ZnO doped with transition metal ions.

In the ‘near’ configuration chains of TM ions are formed in the *ab* planes of ZnO. However, the TM–TM distance (2.249 Å) is large enough to ignore the direct coupling of TM ions. Both in the ‘near’ and the ‘far’ configurations the TM ions are connected by –O–Zn–O– bonds. The different magnetic couplings between the TM ions in the two configurations cannot simply ascribed to the different TM–TM distances; rather, it is closely related to the anisotropy of the electronic structure or the strong directional nature of chemical bonding of ZnO.

4. Conclusion

The electronic structures and magnetic orderings of Cu- and Mn-doped ZnO have been calculated with the B3LYP hybrid functional method. The dispersions of valence and conduction bands of ZnO are similar to *GW* results, but with an improved energy gap. Because of the reduction of self-interaction in B3LYP the exchange splittings between the occupied and unoccupied 3d states are significantly larger than in the LDA calculations. Insulating states, rather than the half-metallic states from LDA calculations, are obtained for $\text{Zn}_{0.875}\text{TM}_{0.125}\text{O}$ (TM = Cu, Mn). The unoccupied Cu 3d states in (Zn, Cu)O are located below the bottom of the host conduction bands, so in n-type ZnO Cu^{1+} ions can be realized. Due to the large exchange splitting in Mn-doped ZnO the unoccupied Mn 3d states are well above the lowest host conduction bands, and thus Mn^{2+} ions are stable in n-type ZnO. In $\text{Zn}_{0.875}\text{Cu}_{0.125}\text{O}$ the ferromagnetic state of the supercell is about 10 meV more stable than the antiferromagnetic,

but for n-type ZnO ferromagnetism may be destroyed by electrons occupying the empty Cu 3d states. In agreement with one of the prior LDA calculations, Mn-doped ZnO has an antiferromagnetic ground state. An Mn clustering effect is predicted.

Acknowledgment

The author would like to thank the computational materials group at Daresbury Laboratory, UK for providing computing resources.

References

- [1] Ohno H 1998 *Science* **281** 951
- [2] See, for example Pearton S J, Abernathy C R, Overberg M E, Thaler G T, Norton D P, Theodoropoulou N, Hebard A F, Park Y D, Ren F, Kim J and Boatner L A 2003 *J. Appl. Phys.* **93** 1
- [3] Prinz G A 1998 *Science* **282** 1660
Wolf S F, Awschalom D D, Buhrman R A, Daughton J M, von Molnar S, Roukes M L, Chtchelkanova A Y and Treger D M 2001 *Science* **294** 1488
Chiba D, Yamanouchi M, Matsukura F and Ohno H 2003 *Science* **301** 943
- [4] See, for example Norton D P, Pearton S J, Hebard A F, Theodoropoulou N, Boatner L A and Wilson R G 2003 *Appl. Phys. Lett.* **82** 239
- [5] Matsumoto Y, Murakami M, Shono T, Hasegawa T, Fukumura T, Kawasaki M, Ahmet P, Chikyow T, Koshihara S and Koinuma H 2001 *Science* **291** 854
- [6] Dietl T, Ohno H, Matsukura F, Cibert J and Ferrand D 2000 *Science* **287** 1019
- [7] Lee H J, Jeong S Y, Cho C R and Park C H 2002 *Appl. Phys. Lett.* **81** 4020
- [8] Norton D P, Pearton S J, Hebard A F, Theodoropoulou N, Boatner L A and Wilson R G 2003 *Appl. Phys. Lett.* **82** 239
- [9] Jung S W, An S J, Yi G C, Jung C U, Lee S I and Cho S 2002 *Appl. Phys. Lett.* **80** 4561
- [10] Han S J, Song J W, Yang C H, Park S H, Park J H, Jeong Y H and Rhite K W 2002 *Appl. Phys. Lett.* **81** 4212
- [11] Cho Y M and Choo W K 2002 *Appl. Phys. Lett.* **80** 3358
- [12] Ueda K, Tabata H and Kawai T 2001 *Appl. Phys. Lett.* **79** 988
- [13] Kim J H, Kim H, Kim D, Ihm Y E and Choo W K 2002 *J. Appl. Phys.* **92** 6066
- [14] Jin Z, Fukumura T, Kawasaki M, Ando K, Saito H, Sekiguchi T, Yoo Y Z, Murakami M, Matsumoto Y, Hasegawa T and Koinuma H 2001 *Appl. Phys. Lett.* **78** 3824
- [15] Fukumura T, Jin Z, Kawasaki M, Shono T, Hasegawa T, Koshihara S and Koinuma H 2001 *Appl. Phys. Lett.* **78** 958
- [16] Sato K and Katayama-Yoshida H 2000 *Japan. J. Appl. Phys.* **39** L555
- [17] Park M S and Min B I 2003 <http://arxiv.org/abs/cond-mat/0307359>
- [18] Spaldin N A 2003 <http://arxiv.org/abs/cond-mat/0306477>
- [19] Mizokawa T, Nambu T, Fujimori A, Fukumura T and Kawasaki M 2002 *Phys. Rev. B* **65** 085209
- [20] Becke A D 1993 *J. Chem. Phys.* **98** 5648
- [21] Muscat J, Wander A and Harrison N M 2001 *Chem. Phys. Lett.* **342** 397
- [22] Bredow T and Gerson A R 2000 *Phys. Rev. B* **61** 5194
- [23] Perry J K, Tahir-Kheli J and Goddard W A III 2001 *Phys. Rev. B* **63** 144510
- [24] Moreira I P R, Illas F and Martin R L 2002 *Phys. Rev. B* **65** 155102
- [25] Feng X B and Harrison N M 2004 *Phys. Rev. B* **69** 132502
- [26] Feng X B and Harrison N M 2004 *Phys. Rev. B* **69** 035114
- [27] Muñoz D, Harrison N M and Illas F 2004 *Phys. Rev. B* **69** 085115
- [28] Usuda M, Hamada N, Kotani T and van Schilfgaarde M 2002 *Phys. Rev. B* **66** 125101
- [29] Massidda S, Resta R, Posternak M and Baldereschi A 1995 *Phys. Rev. B* **52** 16977
- [30] Perdew J P 1991 *Electronic Structure of Solids* ed P Ziesche and H Eschrig (Berlin: Academic)
- [31] Lee L, Yang W and Parr R G 1988 *Phys. Rev. B* **37** 785
- [32] Saunders V R, Dovesi R, Roetti C, Causa M, Harrison N M, Orlando R and Zicovich-Wilson C M 1998 *CRYSTAL98 User's Manual* (Torino: University of Torino)
- [33] http://www.chimifm.unito.it/teorica/crystal/Basis_Sets/mendel.html
- [34] Oshikiri M and Aryasetiawan F 2000 *J. Phys. Soc. Japan* **69** 2123
- [35] Ley L, Pollak R A, McFeely F R, Kowalczyk S P and Shirley D A 1974 *Phys. Rev. B* **9** 600
- [36] Georges A, Kotliar G, Krauth W and Rozenberg M J 1996 *Rev. Mod. Phys.* **68** 13